

Fig. 10a

Fig. 10b

Fig. 10. Profiles of craters produced by clustered pyrex fragments impacting at high velocity (Figure 10a) and low velocity (Figure 10b) into compacted pumice and no. 140-200 sand. In Figure 10a the upper profile (821231) resulted from an impact at 4.8 km/s with a dispersion of 8 cm into compacted pumice, whereas the lower profile (830203) resulted from an impact at 4.35 km/s with identical dispersion into sand. In Figure 10b the upper profile (830526) resulted from a 1.77 km/s impact with a 7.0-cm dispersion into compacted pumice, whereas the lower profile (830608) resulted from a 1.6 km/s impact with an 8.5-cm dispersion into sand. Compacted pumice has greater compressive and shear strength than sand, thereby producing a different morphology. The high-velocity impacts into either compacted pumice or sand tend to produce mounded crater floors for the same dispersion at impact. The crater profiles are scaled such that the apparent diameter is the same with no vertical exaggeration.

apex angle of the principal herringbone ridge decreases from near 45° to near 30° as the impact angle decreases from 45° to 30° (from the horizontal). The higher-velocity (1.5 km/s) broken pyrex impacts into pumice produce the same trend. Figure 17 shows that at a 30° impact angle, the broken pyrex

cluster does not form major herringbone ridges but does form a thick fan zone, which may be equivalent. Minor ridges, however, do extend from the rim with large apex angles. Additionally, Figure 18 indicates that the uprange zone of ejecta avoidance generally becomes wider (i.e., the apex angle

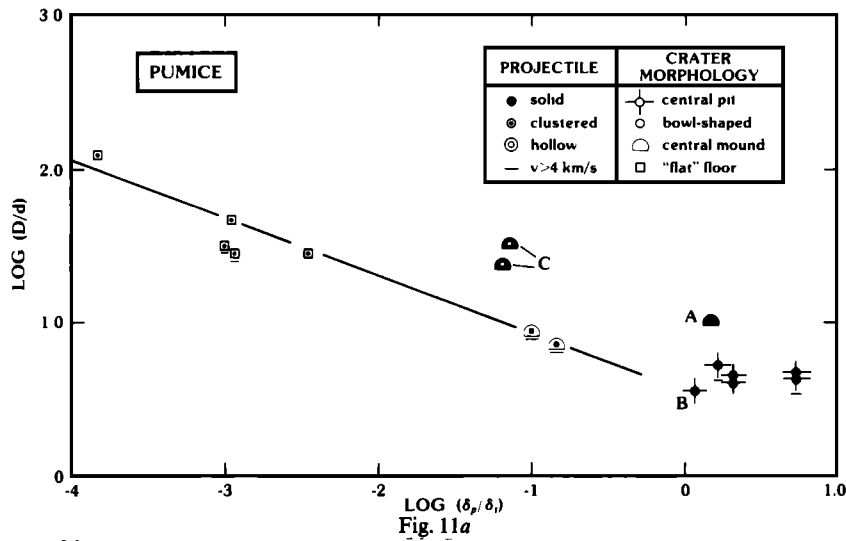


Fig. 11a

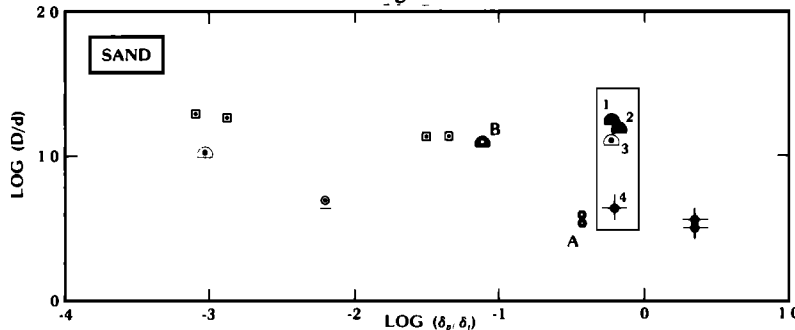


Fig. 11b

Fig. 11. The effect of projectile/target density ratio on the aspect ratio and morphology of impacts into compacted pumice (Figure 11a) and sand (Figure 11b). The aspect ratio (diameter/depth = D/d) decreases for clustered impacts into compacted pumice but is uncorrelated for impacts into sand. Least squares fit for only the clustered impact data into pumice and sand gives, respectively, $\log(D/d) = -0.38 \log(\delta_p/\delta_t) + 0.541$ (correlation coefficient of -0.970) and $\log(D/d) = -0.0398 \log(\delta_p/\delta_t) + 1.016$ (correlation coefficient of -0.167). Identified data points in Figure 11a represent the following impactors: plastically deformable sphere (A), weak and brittle sphere (B), and hollow thin-shelled nylon spheres (C). Identified data points in Figure 11b represent the following: hollow aluminum sphere (A) and a hollow thin-shelled nylon sphere (B). The enclosed numbered data in Figure 11b indicate impacts by a variety of projectile types into moist sand and correspond to identifications in Figure 6.